

Superconductor - Normal and Quantum Superconductor-Insulator Transition at the LaAlO₃/SrTiO₃ Interface

T. Schneider

*Physick-Institute, University of Zurich, Winterthurerstrasse 190, 8057 Zurich, Switzerland. **

A.D. Caviglia, S. Gariglio, N. Reyren, D. Jaccard, and J.-M. Triscone
DPMC, University of Geneva, 24 Quai Ernest-Ansermet, 1211 Geneva 4, Switzerland.

(Dated: November 22, 2018)

Superconductivity at the interface between the insulators LaAlO₃ and SrTiO₃ has been tuned with the electric field effect. The data provide evidence for a two dimensional quantum superconductor to insulator (2D-QSI) transition. Here we explore the compatibility of this phase transition line with Berezinskii-Kosterlitz-Thouless (BKT) behavior and a 2D-QSI transition. In an intermediate regime, limited by a finite size effect, we uncover remarkable consistency with BKT-criticality, weak localization in the insulating state and non-Drude behavior in the normal state. Our estimates for the critical exponents of the 2D-QSI-transition, $z \simeq 1$ and $\bar{\nu} \simeq 2/3$, suggest that it belongs to the 3D-xy universality class.

PACS numbers: 74.78.-w, 74.40.+k, 74.90.+n, 74.78.Fk

The conducting interface between LaAlO₃ and SrTiO₃, two excellent band insulators, has been attracting a lot of attention [1, 2, 3, 4, 5]. Recently, two different ground states, magnetic [6] and superconducting [7], have been experimentally identified. In a very recent report [8], it was shown that the electric field effect can be used to map the phase diagram of this interface system. As the carrier density is increased the system undergoes a 2D-QSI transition. A further increase reveals a superconducting dome. Moreover it was shown that the characteristics of the superconducting transition are consistent with a superconducting sheet of about 10 nm thick [9].

Here we attempt to unravel the nature of the phase transition line and its endpoint which separates the superconducting from the insulating ground state. For this purpose we explore the compatibility of the phase transition with Berezinskii-Kosterlitz-Thouless (BKT) critical behavior [10, 11] and of its endpoint, where superconductivity disappears, with a two dimensional quantum superconductor to insulator (2D-QSI) transition associated with weak localization [12]. In contrast to the disorder tuned QSI transition, electrostatic tuning changes the carrier density without altering the disorder landscape [13]. In an intermediate temperature regime we uncover remarkable agreement with BKT-criticality in the superconductor to normal state transition, weak localization in the insulating phase, and non-Drude behavior in the normal state. It is shown that both conduction mechanisms are limited by a finite size effect, whereupon the BKT-correlation length and the diverging length associated with weak localization [12] cannot grow beyond a limiting length, set by the extent of the homogeneous regions. Our analysis also reveals that the electrostatic tuned BKT-phase transition line ends at a 2D-QSI critical point which appears to fall onto the universality class of the classical 3D-xy model. In addition we explore the

T_c dependence of the vortex core radius and the vortex energy. These properties appear to be basic ingredients to understand the T_c variation.

To explore the compatibility with BKT critical behavior we invoke the characteristic temperature dependence of the correlation length above T_c [11],

$$\xi = \xi_0 \exp\left(2\pi / \left(bt^{1/2}\right)\right), t = |T/T_c - 1|, \quad (1)$$

where ξ_0 is the classical vortex core radius and b is related to the energy needed to create a vortex [14, 15, 16]. Note that b also enters the temperature dependence of the magnetic penetration depth λ below the universal Nelson-Kosterlitz jump: $\lambda^2(T_c)/\lambda^2(T) = (1 + b|t|^{1/2}/4)$ [14]. Moreover, b is related to the vortex energy E_c in terms of [16, 17]

$$b = 4\pi T_c^{1/2}/b_R = f(E_c/(k_B T_c)). \quad (2)$$

Invoking dynamic scaling the resistance R scales in $D = 2$ as [18]

$$R \propto \xi^{-z_{cl}}, \quad (3)$$

where z_{cl} is the dynamic critical exponent of the classical dynamics. z_{cl} is usually not questioned to be anything but the value that describes simple diffusion: $z_{cl} = 2$ [19]. Combining these scaling forms and taking the occurrence of a 2D-QSI transition at $R_{0c} = R_0(T_c = 0)$ into account we obtain

$$R(T) = R_0 \exp\left(-b_R(T - T_c)^{-1/2}\right), \quad (4)$$

with

$$b_R = 4\pi T_c^{1/2}/b, \quad \Delta R_0 = R_{0c} - R_0 \propto 1/\xi_0^2, \quad (5)$$

because ΔR_0 is the singular part of R_0 close to the 2D-QSI transition. To assess the compatibility with the characteristic BKT-behavior we analyze the data in terms of

$$(d \ln R/dT)^{-2/3} = (2/b_R)^{2/3} (T - T_c). \quad (6)$$

Fig. 1 shows $(d \ln R/dT)^{-2/3}$ vs. T for $V_g = 40$ V. V_g is the gate voltage allowing to tune the carrier density. In spite of the rounded transition there is an intermediate regime revealing the characteristic BKT-behavior (6). Noting that real systems are homogeneous over a limited domain only, the rounding may be attributable to a standard finite size effect, whereupon the correlation length cannot grow beyond a limiting length, set by the lateral extent L of the homogenous regions [18, 20]. In this case $R(T)$ scales as $R(T)\exp(b_R |T - T_c|^{-1/2})/R_0 = f(x)$. $f(x)$ is the finite size scaling function with $x = \exp(b_R |T - T_c|^{-1/2})/L^2 \propto \xi^2/L^2$. If $\xi < L$ critical behavior can be observed as long as $f(x) \simeq 1$. This regime corresponds to the horizontal line in the inset of Fig. 1. If $\xi > L$ the scaling function approaches $f(x) \propto x$ so that $R(T)/R_0$ tends to L^{-2} , the behavior indicated by the dashed line. In this context it should be recognized that the BKT correlation length does not exhibit the usual and relatively slow algebraic divergence as T_c is approached (Eq. (1)). For this reason the elimination of the finite size effect would require unprecedented sample homogeneity. The emerging agreement with BKT behavior, limited by a standard finite size effect, allows us to discriminate the rounded transition from other scenarios, including strong disorder which destroys the BKT behavior. It also provides the basis to estimate T_c , $b_R(T_c)$ and $R_0(T_c)$, and with that $b(T_c)$ and $\xi_0 \propto \Delta R_0^{-1/2}$ with reasonable accuracy.

Applying this approach to the $R(T)$ data for each gate voltage V_g we obtain the BKT-transition line depicted in Fig. 2, displayed as T_c vs. $R_\square(T^*)$, the normal state sheet resistance at $T^* = 0.4$ K. We observe that it ends around $R_{\square c} \simeq 4.28$ k Ω where the system is expected to undergo a 2D-QSI transition because T_c vanishes. With reduced R_\square the transition temperature increases and reaches its maximum value, $T_{cm} \simeq 0.31$ K, around $R_\square \simeq 1.35$ k Ω . With further reduced resistance T_c decreases. To identify deviations from Drude behavior ($\sigma \propto n$) in the normal state, which will be discussed later, we also included the gate voltage dependence of the normal state resistance.

According to the scaling theory of quantum critical phenomena one expects that close to the 2D-QSI transition T_c scales as [18, 21]

$$T_c \propto \delta^{z\bar{\nu}}, \quad (7)$$

where δ is the appropriate scaling argument, measuring the relative distance from criticality. $\bar{\nu}$ denotes the critical exponent of the zero temperature correlation length

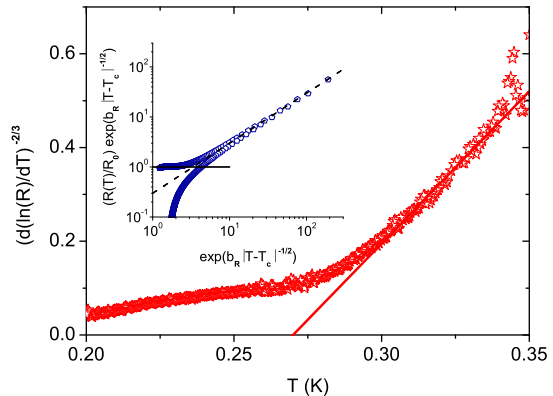


FIG. 1: $(d \ln R/dT)^{-2/3}$ vs. T for $V_g = 40$ V from Caviglia *et al.* [8] where $R = 3/5 R_\square$. The solid line is $(d \ln R/dT)^{-2/3} = 6.5(T - T_c)$ yielding the estimates $T_c = 0.27$ K and $(2/b_R)^{2/3} = 6.5$; the inset shows $R \exp(b_R |T - T_c|^{-1/2})/R_0$ vs. $\exp(b_R |T - T_c|^{-1/2})$ with $R_0 = 1670$ Ω . The upper branch corresponds to $T > T_c$ and the lower one to $T < T_c$. The solid line is $(R/R_0)\exp(b_R |T - T_c|^{-1/2}) = 1$ and the dashed one $(R/R_0)\exp(b_R |T - T_c|^{-1/2}) = 0.4\exp(b_R |T - T_c|^{-1/2}) \propto (\xi/L)^2$.

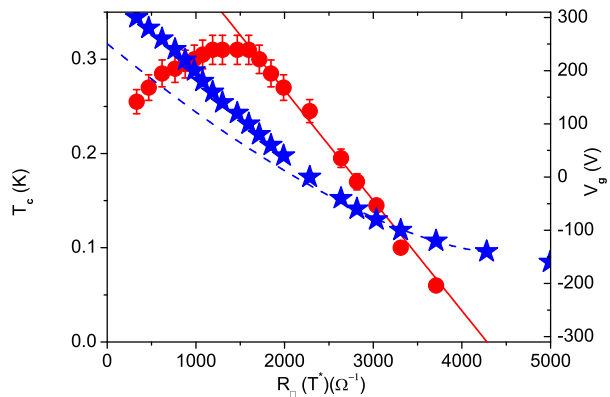


FIG. 2: T_c vs. $R_\square(T^*)$ (\bullet) and V_g vs. $R_\square(T^*)$ (\blackstar) at $T^* = 0.4$ K from Caviglia *et al.* [8]. The solid line is $T_c = 1.17 \cdot 10^{-4} \Delta R(T^*)$ and the dashed one $V_g = V_{gc} + 1.39 \cdot 10^{-3} \Delta R^{3/2}(T^*)$ with $\Delta R(T^*) = (R_{\square c}(T^*) - R_\square(T^*))$, $R_{\square c}(T^*) = 4.28$ k Ω and $V_{gc} = -140$ V.

$\xi(T=0) \propto \delta^{-\bar{\nu}}$ and z the dynamic critical exponent. From Fig. 2 it is seen that the experimental data point to the relationship

$$T_c \propto \Delta R(T^*) \propto \Delta V_g^{2/3}, \quad (8)$$

close to quantum criticality. If the scaling argument is $\Delta R(T^*)$, $z\bar{\nu} = 1$, while if $\delta = \Delta V_g$, $z\bar{\nu} = 2/3$. Since

the measured modulation of the charge density Δn_{2D} induced by the gate voltage scales in the regime of interest as [8]

$$\Delta V_g \propto \Delta n_{2D} \propto T_c^{3/2}, \quad (9)$$

we obtain $z\bar{\nu} = 2/3$ if ΔV_g or Δn_{2D} are taken as scaling argument δ . To identify the correct scaling argument we use the fact that $\delta \propto \Delta n_{2D}$ holds if $(2+z)\bar{\nu} \geq 2$ [22]. To check this inequality, given $z\bar{\nu}$, we need an estimate of z . For this purpose we invoke relation (5), $R_{0c} - R_0(T_c) \propto \xi_0^{-2}(T_c)$ ($z_{cl} = 2$) which diverges as $\xi_0(T_c) \propto \xi(T=0) \propto \delta^{-\bar{\nu}} \propto T_c^{-1/z}$, so that the scaling relation

$$\Delta R_0(T_c) = R_{0c} - R_0(T_c) \propto \xi_0^{-2}(T_c) \propto \delta^{2\bar{\nu}} \propto T_c^{2/z}, \quad (10)$$

holds. Fig. 3 depicts the T_c dependence of $\xi_0(T_c) \propto (R_{0c} - R_0(T_c))^{-1/2}$ and b , which is related to the vortex energy E_c (Eq. (2)). Approaching the 2D-QSI-transition we observe that the data point to $\xi_0(T_c) \propto 1/T_c$, yielding for z the estimate $z \simeq 1$ so that $\bar{\nu} \simeq 2/3$ with $z\bar{\nu} \simeq 2/3$. As these exponents satisfy the inequality $(2+z)\bar{\nu} \geq 2$ [22] we identified the correct scaling argument, $\delta \propto \Delta n_{2D} \propto \Delta V_g$. From the gate voltage dependence of the normal state sheet resistance shown in Fig. 2 it also follows that the normal state conductivity scales as $\Delta\sigma_{\square}(T^*) = \sigma_{\square}(T^*) - \sigma_{\square c}(T^*) \propto \Delta V_g^{2/3}$. The 2D-QSI transition is then characterized by the scaling relations

$$T_c \propto \delta^{2/3} \propto \Delta R(T^*) \propto \Delta R_0^{1/2}(T_c) \propto \Delta V_g^{2/3} \propto \Delta n_{2D}^{2/3} \propto \Delta\sigma_{\square}(T^*) \propto \xi_0^{-1}(T_c), \quad (11)$$

where $\Delta\sigma_{\square}(T^*) \propto \Delta n_{2D}^{2/3}$ reveals non-Drude behavior in the normal state. The product $z\bar{\nu} \simeq 2/3$ agrees with that found in the electric field effect tuned 2D-QSI transition in amorphous ultrathin bismuth films [23] and the magnetic-field-induced 2D-QSI transition in $\text{Nb}_{0.15}\text{Si}_{0.85}$ films [24]. On the contrary it differs from the value $z\bar{\nu} \simeq 1$ that has been found in thin $\text{NdBa}_2\text{Cu}_3\text{O}_7$ films using the electric-field-effect modulation of the transition temperature [25]. In any case our estimates, $z \simeq 1$ and $\bar{\nu} \simeq 2/3$ point to a 2D-QSI transition which belongs to the 3D-xy universality class [18]. Fig. 3 also depicts the T_c dependence of b , which is related to the vortex energy. Since b tends to a constant in the limit $T_c \rightarrow 0$, Eq. (2) implies $db/dT_c = 0$ and therewith $E_c(T_c) \propto k_B T_c$, while the vortex core radius ξ_0 diverges as $\xi_0(T_c) \propto 1/T_c$, in analogy to the behavior of superfluid ^4He films [26]. The 2D-QSI transition is then also characterized by an infinite vortex core radius and vanishing vortex core energy. As T_c increases from the 2D-QSI transition, ξ_0 drops, while the vortex core energy increases. Finally, after passing the maximum T_c the vortex core radius continues to decrease with reduced T_c while b increases further.

Having presented the evidence for an electric field effect tuned BKT line ending at a 2D-QSI-transition belonging

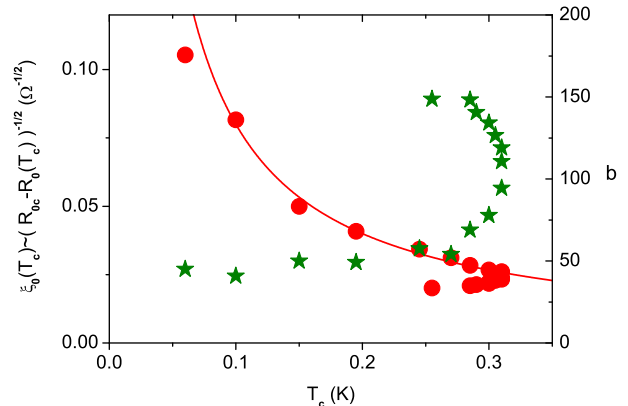


FIG. 3: $\xi_0(T_c) \propto (R_{0c} - R_0(T_c))^{-1/2}$ (●) and b (★) vs. T_c from Caviglia *et al.* [8] where $R = 3/5 R_{\square}$. The solid line is $\xi_0(T_c) \propto (R_{0c} - R_0(T_c))^{-1/2} = 8 \cdot 10^{-3}/T_c$ with $R_{0c} = 2700 \Omega$.

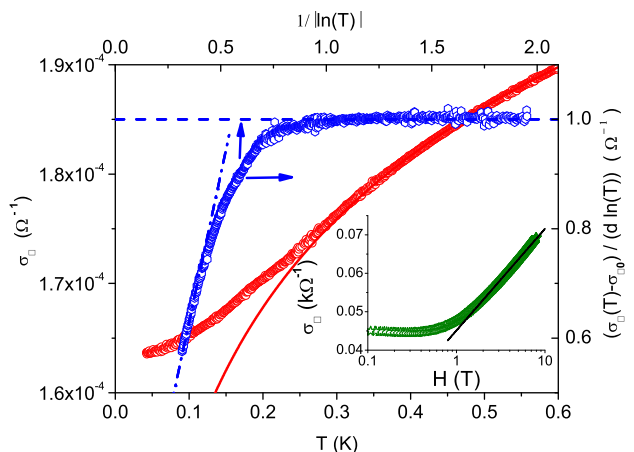


FIG. 4: σ_{\square} vs. T and $(\sigma_{\square}(T) - \sigma_{\square 0}) / (d \ln(T))$ vs. $1/|\ln(T)|$ at $V_g = -240$ V from Caviglia *et al.* [8]. The solid line is $\sigma_{\square}(T) = \sigma_{\square 0} + d \ln(T)$ with $\sigma_{\square 0} = 1.2 \cdot 10^{-4} (\Omega^{-1})$ and $d = 1.2 \cdot 10^{-5} (\Omega^{-1})$, the dashed one $(\sigma_{\square}(T) - \sigma_{\square 0}) / (d \ln(T)) = 1$ and the dash-dot one $(\sigma_{\square}(T) - \sigma_{\square 0}) / d = 1.8 \propto 1/L$. The inset shows the magnetoconductivity σ_{\square} vs. H , applied perpendicular to the interface, at $T = 0.03$ K and $V_g = -300$ V, from Caviglia *et al.* [8]. The solid line is $\sigma_{\square} = 4.51 \cdot 10^{-2} + 1.12 \cdot 10^{-2} \ln(H)$ $\text{k}\Omega^{-1}$.

to the 3D-xy universality class and non-Drude behavior in the normal state an important issue remains, the nature of the insulating phase. Fig. 4 shows the temperature dependence of σ_{\square} for $V_g = -240$ V, which is rather deep in the insulating phase [8]. In analogy to Fig. 1 we observe a rounded transition. In the present case the intermediate regime is compatible with weak localization, $\sigma_{\square}(T) = \sigma_{\square 0} + d \ln(T)$ [12]. Given the evidence for the limiting length L , which prevented the attainment of the superconducting ground state, one suspects that it limits the growth of $\xi_{ld} \propto R_{\square} = 1/\sigma_{\square}$, the di-

verging length associated with localization [12], as well. In this case finite size scaling predicts that $\sigma_{\square}(T)$ scales as $(\sigma_{\square}(T) - \sigma_{\square c}) / (d \ln(T)) = g(y)$ with $y = \xi_{ld}/L \propto 1/(L |\ln(T)|)$. $g(y)$ is the finite size scaling function and tends to 1 for $y < 1$. In this case the approach to the insulating ground state can be seen, while for $y > 1$ the crossover to $g(y) \rightarrow y$ sets in and $\sigma_{\square}(T)$ approaches the finite size dominated regime, where $\sigma_{\square}(T) - \sigma_{\square 0} \propto 1/L$. A glance at Fig. 4 reveals that weak localization combined with the finite size effect describes the data very well. In addition, below $V_g = -300$ V d is independent of V_g and its value $d = 1.2 \cdot 10^{-5} \Omega^{-1}$ is close to $d_e = e^2/(\pi h) \simeq 1.23 \cdot 10^{-5} \Omega^{-1}$, generically attributed to electron-electron interaction [27]. The resulting evidence for weak localization is further substantiated by the observed negative magnetoresistance [8] and in particular by the high field behavior of the conductance depicted in the inset of Fig. 4. There we observe consistency with the characteristic $\ln(H)$ high field behavior [12] and $d\sigma_{\square}/d \ln(H) \simeq 1.12 \cdot 10^{-5} \Omega^{-1}$ is close to the theoretical prediction $d\sigma_{\square}/d \ln(H) = e^2/(\pi h) \simeq 1.23 \cdot 10^{-5} \Omega^{-1}$ [28]. As a result, the failure to observe the superconducting and insulating ground states directly, is attributable to a finite size effect, preventing the respective diverging lengths to grow beyond L . Nevertheless, the finite size scaling analysis and the high field magnetoconductivity provide substantial evidence that these are the appropriate ground states in the homogenous and infinite system.

In summary, we have shown that the electrostatically tuned phase transition line at the $\text{LaAlO}_3/\text{SrTiO}_3$ interface, observed by Caviglia *et al.* [8], is consistent with a BKT-line ending at a 2D-QSI critical point with critical exponents $z \simeq 1$ and $\bar{\nu} \simeq 2/3$, so the universality class of the transition appears to be that of the classical 3D-xy model. The normal state was shown to exhibit non-Drude behavior. To identify the superconducting and insulating ground states from the temperature dependence of the resistance we performed a finite size scaling analysis because the growth of the finite temperature correlation length and the diverging length associated with localization turned out to be limited. Nevertheless, in the insulating state we observed in both, the temperature and magnetic field dependence of the resistance, the characteristic weak localization behavior. Furthermore, we explored the T_c dependence of the vortex core radius and the vortex energy. These properties appear to be basic ingredients to unravel the nature of the variation of T_c . Approaching the 2D-QSI transition the vortex energy tends to zero while the vortex core radius and the localization length diverge so the system is an insulator.

This work was partially supported by the Swiss National Science Foundation through the National Center of Competence in Research, and “Materials with Novel Electronic Properties, MaNEP” and Division II.

* Electronic address: tschnei@physik.unizh.ch

- [1] A. Ohtomo and H. Y. Hwang, *Nature* **427**, 423 (2004).
- [2] S. Okamoto and A. J. Millis, *Nature* **428**, 630 (2004).
- [3] P. R. Willmott *et al.*, *Phys. Rev. Lett.* **99**, 155502 (2007).
- [4] W. Siemons *et al.*, *Phys. Rev. Lett.* **98**, 196802 (2007).
- [5] G. Herranz *et al.*, *Phys. Rev. Lett.* **98**, 216803 (2007).
- [6] A. Brinkman *et al.*, *Nat Mater* **6**, 493 (2007).
- [7] N. Reyren *et al.*, *Science* **317**, 1196 (2007).
- [8] A. D. Caviglia *et al.*, *cond-mat: 0807.0585*.
- [9] N. Reyren *et al.*, in preparation.
- [10] V.L. Berezinskii, *Sov. Phys. JETP* **32**, 493 (1971).
- [11] J. M. Kosterlitz, D. J. Thouless, *J. Phys. C* **6**, 1181 (1973).
- [12] P. A. Lee and T. V. Ramakrishnan, *Rev. Mod. Phys.* **57**, 287 (1985).
- [13] C. H. Ahn *et al.*, *Rev. Mod. Phys.* **78**, 1185 (2006).
- [14] V. Ambegaokar, B. I. Halperin, D. R. Nelson, and E. D. Siggia, *Phys. Rev. B* **21**, 1806 (1980).
- [15] D. Finotello and F. M. Gasparini, *Phys. Rev. Lett.* **55**, 2156 (1985).
- [16] Lindsay M. Steele, Ch. J. Yeager, and D. Finotello, *Phys. Rev. Lett.* **71**, 3673 (1993).
- [17] A. J. Dahm, *Phys. Rev. B* **29**, 484 (1984).
- [18] T. Schneider and J. M. Singer, *Phase Transition Approach to High Temperature Superconductivity* (Imperial College Press, London, 2000).
- [19] S. W. Pierson, M. Friesen, S. M. Ammirata, J. C. Hunicutt and LeRoy A. Gorham, *Phys. Rev. B* **60**, 1309 (1999).
- [20] M. E. Fisher and M. N. Barber, *Phys. Rev. Lett.* **28**, 1516 (1972).
- [21] Kihong Kim and Peter B. Weichman, *Phys. Rev. B* **43**, 13, 583 (1991).
- [22] M. P. A. Fisher, P. B. Weichman, G. Grinstein, and D. S. Fisher, *Phys. Rev. B* **40**, 546 (1988).
- [23] Kevin A. Parendo, K. H. Sarwa B. Tan, A. Bhattacharya, M. Eblen-Zayas, N. E. Staley, and A. M. Goldman, *Phys. Rev. Lett.* **94**, 197004 (2005).
- [24] H. Aubin, C. A. Marrache-Kikuchi, A. Pourret, K. Behnia, L. Bergé, L. Dumoulin, and J. Lesueur, *Phys. Rev. B* **73**, 094521 (2006).
- [25] D. Matthey, N. Reyren, J.-M. Triscone, and T. Schneider, *Phys. Rev. Lett.* **98**, 057002 (2007).
- [26] H. Cho and G. A. Williams, *Phys. Rev. Lett.* **75**, 1562 (1995).
- [27] Ya. M. Blanter, V. M. Vinokur, and L. I. Glazman, *Phys. Rev. B* **73**, 165322 (2006).
- [28] B. L. Altshuler, D. Khmel'nitzkii, A. I. Larkin, and P. A. Lee, *Phys. Rev. B* **22**, 5142 (1980).